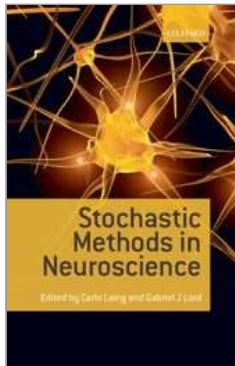


University Press Scholarship Online

Oxford Scholarship Online



Stochastic Methods in Neuroscience

Carlo Laing and Gabriel J Lord

Print publication date: 2009

Print ISBN-13: 9780199235070

Published to Oxford Scholarship Online: February 2010

DOI: 10.1093/acprof:oso/9780199235070.001.0001

Stochastic Dynamic Bifurcations and Excitability

Nils Berglund

Barbara Gentz

DOI:10.1093/acprof:oso/9780199235070.003.0003

Abstract and Keywords

Some models of action potential generation in neurons like the Fitzhugh–Nagumo and the Morris–Lecar model are given by slow–fast differential equations. We outline a general theory allowing us to quantify the effect of noise on such equations. The method combines local analyses around stable and unstable equilibria, and around bifurcation points. We discuss in particular two different mechanisms of excitability, which lead to different types of interspike statistics.

Keywords: action potential generation, stochastic differential equations, slow–fast dynamical systems, dynamic bifurcations, excitability, interspike times, Fitzhugh–Nagumo model, Morris–Lecar model

3.1 Introduction

Neurons communicate through abrupt changes in the electrical potential across their cell membranes, which propagate along axons and transmit information to the synapses of other neurons. Many models for this so-called action-potential generation involve slow–fast dynamical systems. This is due to the fact that the involved variables (flows of ions such as sodium, calcium, and potassium) typically evolve on well-separated time-scales.

One of the first systems of ordinary differential equations describing action-potential generation is a four-dimensional system, which was introduced by Hodgkin and Huxley in 1952 (Hodgkin and Huxley 1952). There exist various two-dimensional systems, obtained either by simplifying the Hodgkin–Huxley system and other models, or simply by fitting experimental data.

Example 3.1 (Morris–Lecar model) This model has been derived to describe giant barnacle (*Balanus Nubilus*) muscle fibres (Morris and Lecar, 1981). It can be written in the form

(3.1)

$$\begin{aligned}\varepsilon \dot{x} &= c_1 m^*(x)(1-x) + c_2 y(V_2 - x) + c_3(V_3 - x), \\ \dot{y} &= (w^*(x) - y)\cosh\left(\frac{x-x_3}{x_4}\right),\end{aligned}$$

where ε is a small parameter, $m^*(x)$ and $w^*(x)$ are the ‘sigmoidal’ functions
(3.2)

$$\begin{aligned}m^*(x) &= \frac{1}{2}\left[1 + \tanh\left(\frac{x-x_1}{x_2}\right)\right], \\ w^*(x) &= \frac{1}{2}\left[1 + \tanh\left(\frac{x-x_3}{x_4}\right)\right],\end{aligned}$$

and the c_i , V_i and x_i are constants.

Example 3.2 (FitzHugh–Nagumo model) This system, which was introduced by FitzHugh (1961) and Nagumo, Arimoto and Yoshizawa (1962) uses the model vector field

(3.3)

$$\begin{aligned}\varepsilon \dot{x} &= x - x^3 + y, \\ \dot{y} &= \alpha - \beta x - \gamma y,\end{aligned}$$

where α , β and γ are constants, and ε is again a small parameter.

(p.66) In this chapter, we discuss methods allowing one to describe quantitatively the effect of noise on slow–fast systems of the form

(3.4)

$$\begin{aligned}\varepsilon \dot{x} &= f(x, y), \\ \dot{y} &= g(x, y),\end{aligned}$$

where $f, g: \mathbb{R}^2 \rightarrow \mathbb{R}$ are (sufficiently smooth) functions. The parameter ε , describing the relative size of the two different time-scales, is assumed to be small, and hence x is called the *fast variable* and y is called the *slow variable*. For simplicity, in the following we will focus on situations where both x and y are one-dimensional. However, many ideas introduced in the (1+1)-dimensional case extend to higher-dimensional systems (Berglund and Gentz, 2003, Berglund and Gentz, 2005).

3.1.1 Fast system, slow manifolds, and nullclines

Deterministic slow–fast systems of the form (3.4) are examples of singularly perturbed systems, which have been extensively studied (for overviews, see for instance the monographs Nayfeh 1973, O’Malley 1974, Wasow 1987, O’Malley 1991 and the proceedings Benoît 1991, Jones 1995).

One way to look at the slow–fast system (3.4) is to slow down time by a factor ε , yielding the equivalent system

(3.5)

$$\begin{aligned}x' &= f(x, y), \\y' &= \varepsilon g(x, y),\end{aligned}$$

where the prime denotes the derivative with respect to the fast time t/ε . This system can then be considered as a small perturbation of the *fast system*, which is the one-parameter family of differential equations

(3.6)

$$x' = f(x, y_0),$$

in which y_0 plays the rôle of a fixed parameter. Being one-dimensional, the asymptotic dynamics of the fast system is typically quite simple: the orbits $x(t)$ converge to one of the equilibrium points of the vector field f , that is, points $x^*_i(y_0)$ such that $f(x^*_i(y_0), y_0) = 0$. Typically they converge to asymptotically stable equilibrium points, i.e. equilibrium points at which the derivative $\partial_x f(x^*_i(y_0), y_0)$ is strictly negative. In exceptional cases (bifurcations), orbits may also converge to points at which $\partial_x f(x^*_i(y_0), y_0)$ vanishes.

The slow–fast system (3.5) can be considered as a perturbation of the fast system (3.6) in which the parameter y moves slowly in time. One expects that orbits will tend to follow the slowly moving stable equilibrium points $x^*_i(y)$. This is why an important rôle is played by the so-called *slow manifolds*, that is, collections of equilibrium points of the fast system, also called *equilibrium branches* in this (1+1)-dimensional context.

(p.67) Another way to see this is by plotting (say) in the (y, x) -plane the *nullclines* of the system, that is, the curves on which $f(x, y) = 0$ or $g(x, y) = 0$. The curves $f(x, y) = 0$ being identical with the slow manifolds, we will henceforth reserve the name nullcline for the curves $g(x, y) = 0$ only. The orbits of the slow–fast system can be sketched with the help of the following rules (Fig. 3.1):

- The equilibrium branches $f(x, y) = 0$ separate the plane into regions where the fast variable x is either increasing or decreasing.
- Away from equilibrium branches, the slope of orbits is large (of order $1/\varepsilon$).
- Orbits which cross equilibrium branches, must cross those horizontally.
- The nullclines $g(x, y) = 0$ separate the plane into regions where the slow variable y is either increasing or decreasing.

- Orbits which cross nullclines, must cross those vertically.
- Intersections of equilibrium branches and nullclines are equilibrium points for the full slow–fast dynamics.

As can be seen in Fig. 3.1, these rules yield orbits tracking stable equilibrium branches with a small delay.

In the models discussed here, the slow manifold is typically S-shaped, that is, it consists of two stable branches and one unstable branch meeting at saddle-node bifurcation points. These points are responsible for the interesting behaviour observed in such systems.

For the FitzHugh–Nagumo model, the slow manifold is given by the equation

(3.7)

$$y = x^3 - x.$$

(p.68) Since
(3.8)

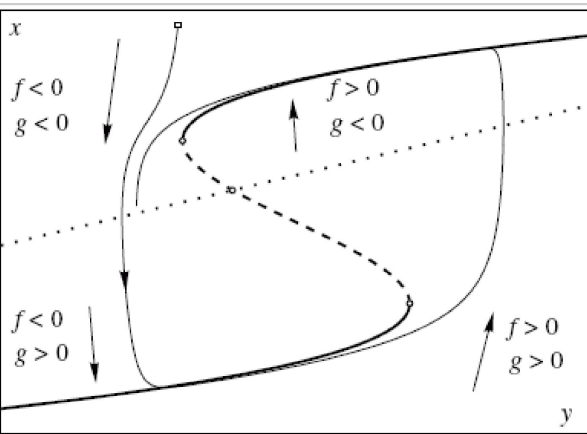


Fig. 3.1: Example of a slow–fast system with stable equilibrium branches (*full heavy curves*), unstable equilibrium branches (*broken heavy curves*), and nullcline (*dotted curve*). The light curve is an orbit of the system, with initial condition marked by a small square. In this example, the system admits a limit cycle.

$$\partial_x f(x, y) = 1 - 3x^2,$$

branches lying in the region $|x| < 1/\sqrt{3}$ are unstable, while branches lying in the region $|x| > 1/\sqrt{3}$ are stable. The saddle-node bifurcation points are located at $(x, y) = \pm(1/\sqrt{3}, -2/3\sqrt{3})$, and the nullcline is simply the straight line

(3.9)

$$\beta x + \gamma y = \alpha$$

For the orrisLecar model, the slow manifold is given by the equation

(3.10)

$$y = -\frac{c_1 m^*(x)(1-x) + c_3(V_3 - x)}{c_2(V_2 - x)},$$

where the stability of its branches depends on the sign of

(3.11)

$$\partial_x f(x, y) = c_1 \partial_x m^*(x)(1-x) - [c_1 m^*(x) + c_2 y + c_3],$$

and the nullcline is given by

(3.12)

$$y = w^*(x)$$

We shall see that the dynamics depends strongly on where the nullclines lie relative to the equilibrium branches.

3.1.2 Models for noise

In the present context of continuous-time slow–fast systems, the simplest mathematical model that can be adopted for noise is additive Gaussian White noise, leading to a system of Itô stochastic differential equations (for the general theory of such equations, see e.g. Øksendal, 1985). This is the situation we will consider here. However, we will allow for the amplitude of the noise terms to depend on the state of the system.

The equations we will consider are thus of the form

(3.13)

$$\begin{aligned} dx(t) &= \frac{1}{\varepsilon} f(x(t), y(t))dt + \frac{\sigma}{\sqrt{\varepsilon}} F(x(t), y(t))dW_t^{(1)}, \\ dy(t) &= g(x(t), y(t))dt + \sigma' G(x(t), y(t))dW_t^{(2)}, \end{aligned}$$

where $W_t^{(1)}$ and $W_t^{(2)}$ are two independent Brownian motions, and $F, G: \mathbb{R}^2 \rightarrow \mathbb{R}$ are two given functions (always assumed to be sufficiently smooth). The small parameters σ and σ' measure the intensity of the two noise terms, in the following sense: During a small time interval Δt , the variance of the noise term for the slow variable grows like $(\sigma')^2 G(x(t), y(t))^2 \Delta t$, while the slow drift term moves the slow variable by $g(x(t), y(t)) \Delta t$ along the orbit. Similarly, the variance of the noise term for the fast variable grows like $\sigma^2 F(x(t), y(t))^2 \Delta t / \varepsilon$, while the fast drift term moves the fast variable by $f(x(t), y(t)) \Delta t / \varepsilon$ along the orbit.

(p.69) The main effect of the noise terms will be that sample paths (which now depend on the realization of the noise) fluctuate in space. As we shall see, near stable equilibrium branches, the size of typical fluctuations is of order σ in the fast direction, and of order σ' in the slow direction, but it may become larger near bifurcation points. Furthermore, transitions between different regions of phase space, which are impossible in the deterministic case, become possible in

the presence of additive noise. Typically, they occur very rarely, on time-scales which are exponentially long in $1/\sigma^2$. However, in the vicinity of bifurcation points, these noise-induced transitions may become much more frequent, thus yielding a dynamics which is qualitatively different from the deterministic one.

The main idea in order to describe the behaviour of solutions of the stochastic system (3.13) is to cut the phase space into several pieces, cf. Fig. 3.2, which are then analysed separately, using different methods. These pieces correspond to:

- the dynamics far from equilibrium branches;
- the dynamics near stable equilibrium branches;
- the dynamics near unstable equilibrium branches;
- the dynamics in the vicinity of bifurcation points.

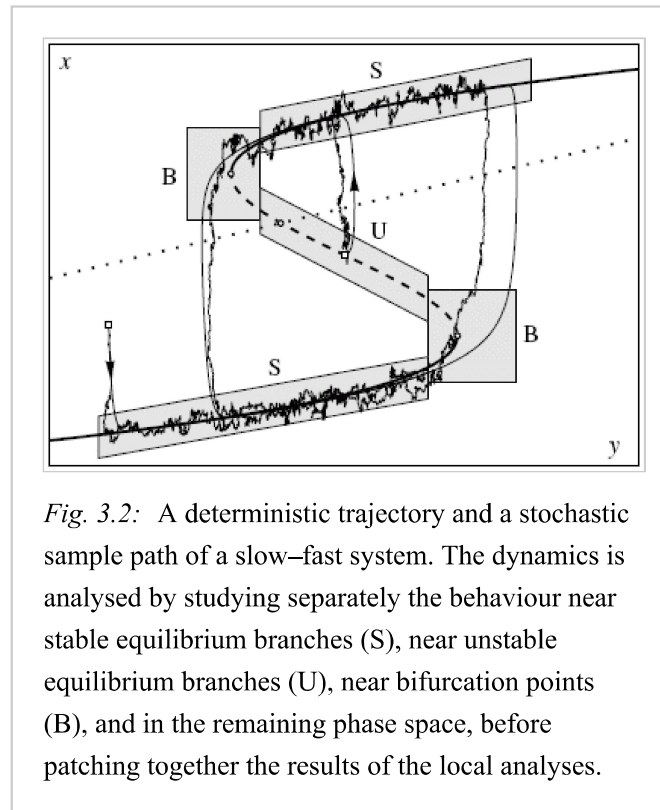
Finally, the global picture is obtained by patching together the results of the different local analyses.

The first situation, namely the dynamics far from equilibrium branches, is quite easily dealt with: In the deterministic case, trajectories have large slopes of order $1/\varepsilon$, and thus usually approach equilibrium branches in a short time of order ε . A rough estimate (Berglund and Gentz, 2005, Theorem 3.1.11) suffices to show that in the stochastic case, sample paths are likely to do the same. We

(p.70) shall thus focus on the dynamics near equilibrium branches, by distinguishing stable branches, unstable branches, and bifurcation points.

Here we limit the discussion to saddle-node bifurcations, because they are the most frequent type of bifurcation in models for neuron dynamics as considered here.

However, similar



ideas can be applied to pitchfork bifurcations (Berglund and Gentz, 2002 *c*), to (avoided) transcritical bifurcations (Berglund and Gentz, 2002 *d*), and to Hopf bifurcations (Berglund and Gentz, 2005, Section 5.3.2).

Let us finally point out that one can be interested in various other types of noise, including

- the same noise acting on slow and fast variables;
- coloured noise, described by an Ornstein–Uhlenbeck process;
- other types of time-correlated noise, derived, for instance, from fractional Brownian motion;
- noise including jumps, derived, from instance, from Lévy processes.

The first two types of noise can be accommodated by an analogous framework, possibly by augmenting the dimension of phase space, see in particular (Berglund and Gentz, 2002 *a*). The other two cases are at the moment much less well understood, and new methods are required in order to quantify their effect.

A major interest of a quantitative study of the effects of different types of noise on the dynamics is that it may help to select the best model for noise relevant in a particular system, by comparison with experimental results.

3.2 Stable equilibrium branches

3.2.1 Deterministic case

We consider general slow–fast systems of the form

(3.14)

$$\begin{aligned}\varepsilon \dot{x} &= f(x, y), \\ \dot{y} &= g(x, y),\end{aligned}$$

for functions $f, g: \mathbb{R}^2 \rightarrow \mathbb{R}$ (always assumed in the sequel to be as smooth as required by the Taylor expansions used in the analysis). We start by considering the dynamics near stable equilibrium branches, that is, collections of asymptotically stable equilibrium points of the associated fast system $\dot{x} = r(x, y_0)$.

Definition 3.3 Assume there exists an interval $I \subset \mathbb{R}$ and a continuous function $x^*: I \rightarrow \mathbb{R}$ such that

(3.15)

$$f(x^*(y), y) = 0 \quad \forall y \in I.$$

Then the set $\mathcal{M}_0 = \{(x^*(y), y) : y \in I\}$ is called an equilibrium branch of the system

(3.14). Let

(3.16)

$$a^*(y) = \partial_x f(x^*(y), y)$$

(p.71) be the linearisation of the fast vector field at $x^*(y)$. The equilibrium branch is called (asymptotically) stable if $a^*(y)$ is negative and bounded away from zero, uniformly in $y \in I$.

A first result, due to Tihonov, states that orbits, starting sufficiently close to a stable equilibrium branch, tend to track that branch up to a small lag of order ε .

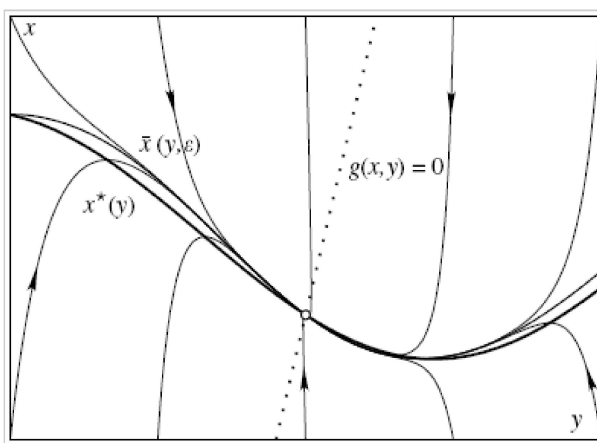


Fig. 3.3: Deterministic dynamics near a stable equilibrium branch $x^(y)$ (full heavy curve), intersecting a nullcline (dotted line). Orbits are attracted exponentially fast by an invariant curve $x = \bar{x}(y, \varepsilon)$, lying at a distance of order ε of the equilibrium branch (in this example $\varepsilon = 0.1$).*

Theorem 3.4 (Tihonov 1952, Gradštejn 1953) *Any orbit starting in a sufficiently small neighbourhood of a stable equilibrium branch \mathcal{M}_0 is attracted exponentially fast to a neighbourhood of order ε of \mathcal{M}_0 .*

A second result, due to Fenichel, makes the picture more precise. It states that all orbits starting near the stable equilibrium branch actually converge to an invariant curve, cf. Fig.3.3.

Theorem 3.5 (Fenichel 1979) *If the equilibrium branch \mathcal{M}_0 is stable, then there exists a curve \mathcal{M}_ε , which is ε -close to \mathcal{M}_0 and invariant under the flow.¹ The curve \mathcal{M}_ε attracts neighbouring orbits exponentially fast.*

The invariant curve \mathcal{M}_ε admits a parametric equation of the form $x = \bar{x}(y, \varepsilon)$, where $\bar{x}(y, \varepsilon) = x^*(y) + \mathcal{O}(\varepsilon)$. The function $\bar{x}(y, \varepsilon)$ can be computed perturbatively in ε to any desired accuracy. Indeed, substituting in (3.14), we obtain the invariance condition

(3.17)

$$f(\bar{x}(y, \varepsilon), y) = \varepsilon \partial_y \bar{x}(y, \varepsilon) g(\bar{x}(y, \varepsilon), y).$$

(p.72) Looking for a solution in the form of an asymptotic series
(3.18)

$$\bar{x}(y, \varepsilon) = x_0(y) + \varepsilon x_1(y) + \varepsilon^2 x_2(y) + \dots$$

(where the existence of such an asymptotic series follows from the centre manifold theorem), we start by inserting the ansatz (3.18) into (3.17). Expanding into powers of ε , and equating like powers allows us to determine the $x_i(y)$. To order ε^0 , one simply gets

(3.19)

$$f(x_0(y), y) = 0,$$

which is the equation defining the equilibrium branch, so that $x_0(y) = x^*(y)$ follows.

To order ε^1 , we obtain

(3.20)

$$\partial_x f(x^*(y), y) x_1(y) = \partial_y x^*(y) g(x^*(y), y).$$

The term $\partial_x f(x^*(y), y)$ is the one we denoted $a^*(y)$, so that

(3.21)

$$x_1(y) = \frac{\partial_y x^*(y) g(x^*(y), y)}{a^*(y)}.$$

Since $a^*(y)$ is negative for the stable equilibrium branch \mathcal{M}_0 , the invariant curve lies below $x^*(y)$ if $x^*(y)$ is increasing and g is positive, while it lies above $x^*(y)$ if $x^*(y)$ is increasing and g is negative (and vice versa for decreasing $x^*(y)$). If g vanishes at a point $(x^*(y^*), y^*)$, then this point is in fact an equilibrium point of the slow–fast system. Hence \mathcal{M}_ε may contain equilibrium points, and if so, it can consist of stable or unstable manifolds of such points.

The dynamics on the invariant curve \mathcal{M}_ε is governed by the reduced equation

(3.22)

$$\dot{y} = g(\bar{x}(y, \varepsilon), y).$$

Expanding in ε , we can write this equation as

(3.23)

$$\begin{aligned} \dot{y} &= g(x^*(y), y) + \varepsilon \partial_x g(x^*(y), y) x_1(y) + \dots \\ &= g(x^*(y), y) \left[1 + \varepsilon \partial_x g(x^*(y), y) \frac{\partial_y x^*(y)}{a^*(y)} + \dots \right]. \end{aligned}$$

We recover the fact that orbits on the invariant curve move to the right if g is positive, and to the left if g is negative.

3.2.2 Stochastic case

We consider now the dynamics of Itô stochastic differential equations of the form

(3.24)

$$\begin{aligned} dx(t) &= \frac{1}{\varepsilon} f(x(t), y(t)) dt + \frac{\sigma}{\sqrt{\varepsilon}} F(x(t), y(t)) dW_t^{(1)}, \\ dy(t) &= g(x(t), y(t)) dt + \sigma' G(x(t), y(t)) dW_t^{(2)}, \end{aligned}$$

(p.73) cf. (3.13), near a stable equilibrium branch. In the first step, we aim at bounds on the deviation

(3.25)

$$\xi(t) = x(t) - \bar{x}(y(t), \varepsilon)$$

of the random fast variables from the deterministic invariant curve. By Itô's formula, this deviation satisfies the stochastic differential equation

(3.26)

$$d\xi(t) = dx(t) - \partial_y \bar{x}(y(t), \varepsilon) dy(t) - \frac{1}{2} \partial_{yy} \bar{x}(y(t), \varepsilon) (dy(t))^2,$$

where $(dy(t))^2$ is to be computed according to the rules of Itô calculus, yielding

(3.27)

$$\begin{aligned} d\xi(t) = & \frac{1}{\varepsilon} f(x(t), y(t)) dt + \frac{\sigma}{\sqrt{\varepsilon}} F(x(t), y(t)) dW_t^{(1)} \\ & - \partial_y \bar{x}(y(t), \varepsilon) g(x(t), y(t)) dt - \partial_y \bar{x}(y(t), \varepsilon) \sigma' G(x(t), y(t)) dW_t^{(2)} \\ & - \frac{1}{2} \partial_{yy} \bar{x}(y(t), \varepsilon) (\sigma')^2 G(x(t), y(t))^2 dt. \end{aligned}$$

Because of the invariance condition (3.17), the coefficient of dt in the above equation vanishes to leading order for $\xi(t)=0$. Expanding everything in $\xi(t)$, one obtains an equation of the form

(3.28)

$$\begin{aligned} d\xi(t) = & \frac{1}{\varepsilon} [\bar{a}(y(t), \varepsilon) \xi(t) + \mathcal{O}(\xi(t)^2) + \mathcal{O}(\varepsilon(\sigma')^2)] dt \\ & + \frac{\sigma}{\sqrt{\varepsilon}} [F_0(y(t), \varepsilon) + \mathcal{O}(\xi(t))] dW_t^{(1)} \\ & - \sigma' \partial_y \bar{x}(y(t), \varepsilon) [G_0(y(t), \varepsilon) + \mathcal{O}(\xi(t))] dW_t^{(2)}, \end{aligned}$$

where we have used the shorthand

(3.29)

$$\begin{aligned} \bar{a}(y, \varepsilon) &= \partial_x f(\bar{x}(y, \varepsilon), y) = a^*(y) + \mathcal{O}(\varepsilon), \\ F_0(y, \varepsilon) &= F(\bar{x}(y, \varepsilon), y) = F(x^*(y), y) + \mathcal{O}(\varepsilon), \\ G_0(y, \varepsilon) &= G(\bar{x}(y, \varepsilon), y) = G(x^*(y), y) + \mathcal{O}(\varepsilon). \end{aligned}$$

The idea is now to choose a suitable Gaussian approximation for ξ . Such an approximation can be obtained by approximating the slow variable $y(t)$ by a deterministic variable $y^0(t)$, while choosing a linear approximation $\xi^0(t)$ for $\xi(t)$, yielding the system

(3.30)

$$\begin{aligned} d\xi^0(t) = & \frac{1}{\varepsilon} \bar{a}(y^0(t), \varepsilon) \xi^0(t) dt + \frac{\sigma}{\sqrt{\varepsilon}} F_0(y^0(t), \varepsilon) dW_t^{(1)} \\ & - \sigma' \partial_y \bar{x}(y^0(t), \varepsilon) G_0(y^0(t), \varepsilon) dW_t^{(2)}, \\ dy^0(t) = & g(\bar{x}(y^0(t), \varepsilon), y^0(t)) dt. \end{aligned}$$

(p.74) Assuming that $x(t)$ starts on $\bar{x}(y(t), \varepsilon)$ at time $t = 0$, it follows that $\xi(0) = 0$, and thus we may also assume that $\xi^0(0) = 0$. Therefore, the process $\{\xi^0(t)\}_t$ is Gaussian with zero mean and variance $\sigma^2 v(t)$, where $v(t)$ can be written as an integral, but also as a solution of the deterministic slow–fast system

(3.31)

$$\begin{aligned}\varepsilon \dot{v}(t) &= 2\bar{a}(y^0(t), \varepsilon)v(t) + F_0(y^0(t), \varepsilon)^2 + \varepsilon \left[\frac{\sigma'}{\sigma} \partial_y \bar{x}(y^0(t), \varepsilon) G_0(y^0(t), \varepsilon) \right]^2, \\ \dot{y}^0(t) &= g(\bar{x}(y^0(t), \varepsilon), y^0(t)).\end{aligned}$$

By Tikhonov's theorem, we conclude that $v(t)$ approaches exponentially fast a function $\bar{v}(y^0(t), \varepsilon)$ satisfying (if we assume $\sigma' \leq \text{const } \sigma$)
(3.32)

$$\bar{v}(y^0(t), \varepsilon) = -\frac{F_0(y^0(t), \varepsilon)^2}{2\bar{a}(y^0(t), \varepsilon)} + \mathcal{O}(\varepsilon).$$

This result is not surprising: It means that the variance of the deviation $\xi^0(t)$ is proportional to the instantaneous variance increase of the noise term, and inversely proportional to the attractivity of the stable equilibrium branch.

The main result is that sample paths of the nonlinear equation are concentrated in a neighbourhood of order $\sigma\sqrt{\bar{v}(y, \varepsilon)}$ of the deterministic invariant curve $\bar{x}(y, \varepsilon)$, provided the diffusion coefficient F is bounded away from zero. We formulate this concentration result by introducing the family of sets

(3.33)

$$\mathcal{B}(h) = \left\{ (x, y) : y \in I, |x - \bar{x}(y, \varepsilon)|^2 < h^2 \bar{v}(y, \varepsilon) \right\}.$$

Each $\mathcal{B}(h)$ is a strip around the deterministic invariant curve, of width proportional to the parameter h and to the standard deviation of the linearized process.

We further introduce two first-exit times:

(3.34)

$$\begin{aligned}\tau_{\mathcal{B}(h)} &= \inf \{t > 0 : (x(t), y(t)) \notin \mathcal{B}(h)\}, \\ \tau_I &= \inf \{t > 0 : y(t) \notin I\}.\end{aligned}$$

Both times are random as they depend on the realization of the sample path $(x(t), y(t))$. While τ_I describes the first time the slow variable is found outside the interval of existence of the equilibrium branch, $\tau_{\mathcal{B}(h)}$ gives the first time the sample path exits the strip $\mathcal{B}(h)$, in which we expect sample paths to be concentrated, cf. Fig. 3.4.

The following result states that indeed, for $h \gg \sigma$, sample paths are unlikely to leave $\mathcal{B}(h)$ – unless $y(t)$ leaves the interval I in which the equilibrium branch is defined.

(p.75)

Theorem 3.6

(Berglund and Gentz 2003)

Assume the initial condition lies on the invariant curve, that is, $x(0) = \bar{x}(y(0), \varepsilon)$ for

some $y(0) \in I$.
 Then there exist constants $h_0, c, L > 0$ such that for all $h \leq h_0$,

(3.35)

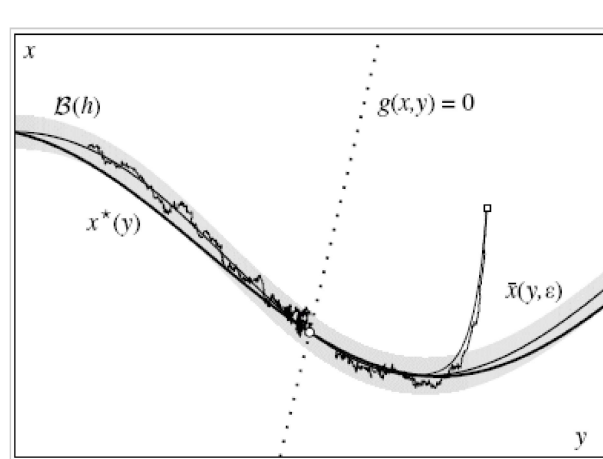


Fig. 3.4: Stochastic dynamics near a stable equilibrium branch $x^*(y)$ (full heavy curve), for the same system as in Fig. 3.3 and noise intensities $\sigma = \sigma' = 0.03$. Sample paths are likely to stay in the shaded set $\mathcal{B}(h)$, centred in the curve $\bar{x}(y, \varepsilon)$ (shown here for $h = 3$). Sample paths starting away from the invariant curve stay close to the deterministic solution starting at the same point. Once the deterministic solution and the random sample path have entered the set $\mathcal{B}(h)$, we may continue to study the sample path as if it had started in $\mathcal{B}(h)$.

$$\Pr(\tau_{\mathcal{B}(h)} < \min(t, \tau_I)) \leq C(t, \varepsilon) e^{-\kappa h^2/2\sigma^2},$$

where the exponent κ is uniform in time and satisfies

(3.36)

$$\kappa = 1 - \mathcal{O}(h) - \mathcal{O}(\varepsilon(\sigma'/h)^2) - \mathcal{O}(e^{-c/\varepsilon}/h),$$

and the prefactor satisfies

(3.37)

$$C(t, \varepsilon) = L \frac{(1+t)^2}{h^2 \varepsilon} \left(1 + \frac{h^2}{\sigma^2} \right)$$

As soon as we take h slightly larger than σ , say $h = \text{const } \sigma |\log \sigma|$, the right-hand side of (3.35) becomes very small, unless we wait for very long time spans. For brevity, we will say that sample paths are concentrated in $\mathcal{B}(\sigma)$.

Remark 3.7

1. A matching lower bound for the probability in (3.35), with an exponent differing only in the error terms, and a different prefactor holds, cf. (Berglund and Gentz, 2003, Theorem 2.4), showing that the

above bound is sharp in the sense that it captures the correct behaviour of the probability.

(p.76)

2. If the sample path does not start on the invariant curve, but in a sufficiently small neighbourhood of the invariant curve, the upper bound (3.35) remains valid, provided we first wait for a time of order $\varepsilon|\log h|$, after which the sample path is likely to have entered $\mathcal{B}(h)$.
3. We expect the exact prefactor of the probability in (3.35) to grow linearly with time t . This has been established in some particular situations, cf. (Berglund and Gentz 2005, Section 3.1).
4. One can show that on a suitable time-scale, the dynamics is well approximated by its projection on the invariant curve, given by

(3.38)

$$dy(t) = g(\bar{x}(y(t), \varepsilon), y(t))dt + \sigma' G(\bar{x}(y(t), \varepsilon), y(t))dW_t^{(2)}$$

5. Note that if the deterministic solution $y^0(t)$ of the deterministic reduced equation $\dot{y}^0 = g(\bar{x}(y^0, \varepsilon), y^0)$ leaves the interval of existence I in a time of order 1, then sample paths of the stochastic equation are likely to leave I in a comparable time, cf. Berglund and Gentz (2003, Theorem 2.6) and Berglund and Gentz (2005, Section 5.1.4).

3.3 Unstable equilibrium branches

3.3.1 Deterministic case

We return to the study of deterministic slow–fast systems of the form (3.14), this time focusing on the dynamics near unstable equilibrium branches.

Definition 3.8 Let $\mathcal{M}_0 = \{(x^*(y), y)\} \{y \in I\}$ be an equilibrium branch of the system (3.14), with linearisation $a^*(y)$ of the fast drift term. The equilibrium branch is called unstable if $a^*(y)$ is positive and bounded away from zero, uniformly in $y \in I$.

In this case, Tikhonov's theorem can still be applied, by looking backwards in time. Simply note that an orbit passing through a point chosen close to the equilibrium branch will approach an ε -neighbourhood of this branch when viewed backwards in time.

Again by looking backwards in time, we see that Fenichel's theorem also holds in the unstable case, i.e. there exists an invariant curve \mathcal{M}_ε in a neighbourhood of order ε of the equilibrium branch. The only difference is that this curve is now repelling neighbouring orbits exponentially fast (looking forward in time). The invariance condition is the same as before, and thus the invariant curve still has an equation of the form $x = \bar{x}(y, \varepsilon)$, where

(3.39)

$$\bar{x}(y, \varepsilon) = x^*(y) + \frac{\partial_y x^*(y)g(x^*(y), y)}{a^*(y)}\varepsilon + \mathcal{O}(\varepsilon^2).$$

Since $a^*(y)$ is now positive, the invariant curve lies above the equilibrium branch if $x^*(y)$ is increasing and g is positive, while it lies below if $x^*(y)$ is increasing and g is negative (and vice versa for decreasing $x^*(y)$).

(p.77) If the initial condition lies at a distance δ_0 from the invariant curve, then the distance will grow roughly like $\delta_0 e^{\text{const}/\varepsilon}$. The time needed to reach a distance δ from the curve is of order $\varepsilon \log(\delta/\delta_0)$, which can be large for very small δ_0 . Hence, though most orbits are quickly repelled from the invariant curve, one can always find orbits staying near the curve for a long time.

3.3.2 Stochastic case

When noise is added to the slow–fast system, sample paths starting on the deterministic curve or close to it typically leave its vicinity earlier than they would in the deterministic case. This is due to the diffusion term being likely to push sample paths to regions where the drift term is sufficiently large to take over and accelerate the escape.

More precisely, assuming the diffusion coefficient $F(x,y)$ is bounded away from zero near the unstable equilibrium branch, one can show (Berglund and Gentz 2005, Section 3.2) that the following holds:

- Let $\rho(y, \varepsilon) = F_0(y, \varepsilon)/\sqrt{2\bar{a}(y, \varepsilon)}$, where F_0 and \bar{a} are defined as in (3.29). For $h \leq \sigma$, sample paths starting on the invariant curve $\bar{x}(y, \varepsilon)$ are likely to leave a neighbourhood of size $h\rho(y, \varepsilon)$ of this curve in a time of order $\varepsilon h^2/\sigma^2$.
- For small δ up to order 1 in σ , sample paths are likely to leave a neighbourhood of size δ of $\bar{x}(y, \varepsilon)$ in a time of order $\varepsilon \log(\delta/\sigma)$.

Hence, sample paths starting at a distance δ_0 from the invariant curve are likely to reach a distance δ in a time of order $\varepsilon \log(\delta/\max(\delta_0, \sigma))$. Thus the system behaves as if the noise term accounts for an effective initial condition at distance σ from the invariant curve.

3.4 Saddle-node bifurcations

3.4.1 Deterministic case

We consider now the dynamics of the deterministic slow–fast system (3.4) near saddle-node bifurcation points.

Definition 3.9 A point (x^*, y^*) is a saddle-node bifurcation point if the fast vector field satisfies the conditions

(3.40)

$$\begin{aligned}
f(x^*, y^*) &= 0, & (\text{equilibrium point}), \\
\partial_x f(x^*, y^*) &= 0, & (\text{bifurcation point}), \\
\partial_{xx} f(x^*, y^*) &\neq 0, & (\text{saddle-node bifurcation}), \\
\partial_y f(x^*, y^*) &\neq 0, & (\text{saddle-node bifurcation}).
\end{aligned}$$

(p.78) In this section, we further assume that

(3.41)

$$g(x^*, y^*) \neq 0, (\text{non-zero slow drift speed}).$$

Cases in which $g(x^*, y^*)$ vanishes, or nearly vanishes, will be considered in the next section.

One can always translate the origin of the coordinate system to the bifurcation point, which amounts to assuming that $(x^*, y^*) = (0, 0)$. One can further scale x, y and time in such a way that $|\partial_{xx} f(0, 0)| = 2$, $|\partial_y f(0, 0)| = 1$ and $|g(0, 0)| = 1$, as in the simple example

(3.42)

$$\begin{aligned}
\varepsilon \dot{x} &= y - x^2, \\
\dot{y} &= -1.
\end{aligned}$$

This system, which is actually the normal form of (3.14) near a saddle-node bifurcation, admits a stable equilibrium branch $x_-^*(y) = \sqrt{y}, y > 0$, with linearisation $a_-^*(y) = -2\sqrt{y}$, and an unstable equilibrium branch $x_+^*(y) = -\sqrt{y}, y > 0$, with linearization $a_+^*(y) = 2\sqrt{y}$, cf. Fig. 3.5. General systems satisfying (3.40) and (3.41) admit branches with the same asymptotic behaviour as $y \rightarrow 0$, possibly with different signs.

Let us stick to Eqn. (3.42) for simplicity. We know that there exists an invariant curve $x = \bar{x}_-(y, \varepsilon)$ tracking $x_-^*(y)$. A computation shows that it satisfies

(3.43)

$$\bar{x}_-(y, \varepsilon) = \sqrt{y} + \frac{\varepsilon}{4y} - \frac{5}{32} \frac{\varepsilon^2}{y^{5/2}} + \mathcal{O}(\varepsilon^3),$$

(p.79) as long as y is bounded away from zero. As y decreases, however, the expansion becomes ‘disordered’: all terms are of comparable size for $y = \varepsilon^{2/3}$, and the expansion is no longer a valid

asymptotic series for $y < \varepsilon^{2/3}$. The curve $\bar{x}_-(y, \varepsilon)$, however, continues to exist, since it can be defined as a particular solution of the slow–fast differential equation. Its fate is described by the following general result (Pontryagin 1957, Haberman 1979, Berglund and Kunz 1999).

Theorem 3.10 Let (x^*, y^*) be a saddle-node bifurcation point of a slow–fast system satisfying (3.41). Assume (without loss of generality) that the coordinates have been scaled in such a way that $(x^*, y^*) = (0, 0)$, $\partial_{xx} f(0, 0) = -2$, $\partial_y f(0, 0) = -1$ and $g(0, 0) = -1$. Choose an initial condition $(x(0), y(0))$ sufficiently close to the bifurcation point, with $y(0) > 0$ of order 1 and $x(0) - x^*(y(0)) > 0$ of order ε . Then the orbit starting in $(x(0), y(0))$ satisfies²

(3.44)

$$\begin{aligned} x(t) - x_-(y(t)) &\asymp \frac{\varepsilon}{y(t)} \text{ for } c_1 \varepsilon^{2/3} \leq y(t) \leq y(0), \\ x(t) &\asymp \varepsilon^{1/3} \text{ for } -c_1 \varepsilon^{2/3} \leq y(t) \leq c_1 \varepsilon^{2/3}, \end{aligned}$$

for some constant $c_1 > 0$. Furthermore, $x(t)$ reaches negative values of order 1 when $y(t)$ is still of order $-\varepsilon^{2/3}$.

This result implies that when continued from positive to negative y , the invariant curve $x = \bar{x}_-(y, \varepsilon)$ first crosses the axis $y=0$ for an x of order $\varepsilon^{1/3}$, then the axis $x=0$ for a y of order $-\varepsilon^{2/3}$, and finally reaches negative x of order 1, still for a y of order $-\varepsilon^{2/3}$ (Fig. 3.5.).

3.4.2 Stochastic case

We turn now to the behaviour of the stochastic differential equation (3.13) near a saddle-node bifurcation point, which we assume to lie at $(0, 0)$. We further assume that

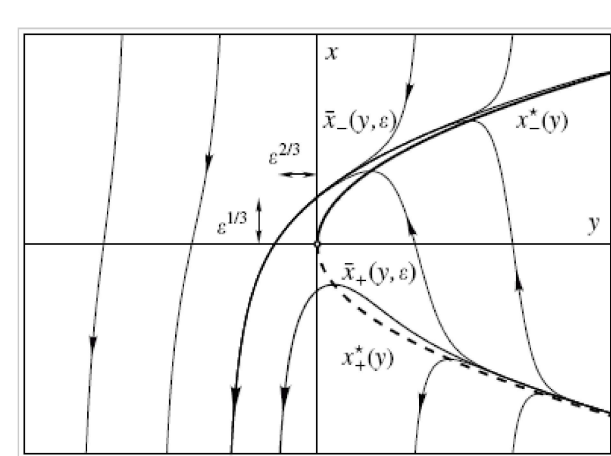


Fig. 3.5: Some orbits of the deterministic slow–fast system (3.42) describing the dynamics near a saddle-node bifurcation point, for $\varepsilon = 0.1$. The invariant curve $x = \bar{x}_-(y, \varepsilon)$, tracking the stable branch $x = x^*_-(y)$ for positive y , crosses the x -axis at a distance of order $\varepsilon^{1/3}$ above the origin, and the y -axis at a distance of order $\varepsilon^{2/3}$ to the left of the origin. Also shown is the invariant curve $x = \bar{x}_+(y, \varepsilon)$, tracking the unstable branch $x = x^*_+(y)$ for positive y .

(3.45)

$$F(0,0) \neq 0 (\text{non-zero noise on fast component}).$$

By continuity, F will be non-zero in a full neighbourhood of the bifurcation point. One can try to proceed as in the stable case, and define a neighbourhood $\mathcal{B}(h)$ of the invariant curve $\bar{x}_-(y, \varepsilon)$ tracking the stable equilibrium branch $x^*_-(y)$, cf. (3.33). The new feature is that the function $\bar{v}(y, \varepsilon)$ controlling the variance of fluctuations, defined as the solution of the system (3.31), does not remain of **(p.80)** order 1. In fact, Theorem 3.10 implies that $\bar{a}(y, \varepsilon) = \partial_x f(\bar{x}_-(y, \varepsilon), y)$ scales like $\max(y^{1/2}, \varepsilon^{1/3})$ and hence

(3.46)

$$\bar{v}(y, \varepsilon) \asymp \frac{1}{\max(y^{1/2}, \varepsilon^{1/3})}$$

for $y \geq -c_1 \varepsilon^{2/3}$. It follows that the set $\mathcal{B}(h)$ becomes wider as $y(t)$ approaches the bifurcation point, and reaches a width of order $h\varepsilon^{-1/6}$ near $y=0$.

If $\sigma < \varepsilon^{1/2}$, we can choose an h satisfying $\sigma < h < \varepsilon^{1/2}$. For such h , the width of $\mathcal{B}(h)$ is still smaller than the distance to the bifurcation point, which has order $\varepsilon^{1/3}$. In this situation, the results of Theorem 3.6 remain valid, and sample paths are concentrated in the corresponding set $\mathcal{B}(h)$ as long as $y(t) > -c_1 \varepsilon^{2/3}$ (Fig. 3.6a).

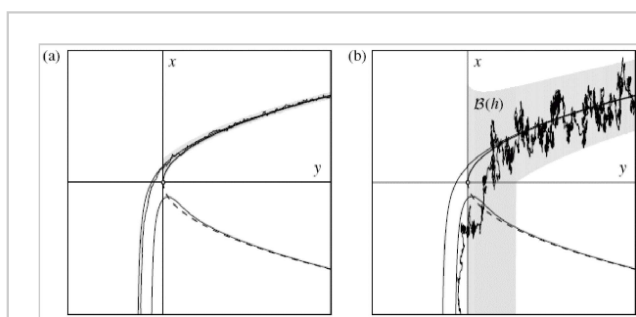
If $\sigma > \varepsilon^{1/2}$, fluctuations already allow sample paths to reach the unstable branch as soon as $y(t)$ has decreased to order $\sigma^{4/3}$. One then shows that sample paths are likely to overcome the unstable branch, and to reach negative x -values of order 1, for only slightly smaller y , cf. Fig. 3.6(b). These results can be summarized as follows.

Theorem 3.11 (Berglund and Gentz 2002b) *Assume the conditions of Theorem 3.10 hold, as well as (3.45), and that $\sigma' \leq \text{const } \sigma$. Then the following hold:*

- If $\sigma < \sigma_c = \varepsilon^{1/2}$, then sample paths remain in $\mathcal{B}(h)$ with probability larger than $1 - O(e^{-h^2/2\sigma^2})$ for all h up to order $\varepsilon^{1/2}$, as long as $y(t) > -c_1 \varepsilon^{2/3}$. In particular, the probability that $x(t)$ becomes negative for these $y(t)$ is of order $e^{-O(\varepsilon/\sigma^2)}$. Furthermore, $x(t)$ is likely to reach negative values of order 1 as soon as $y(t)$ reaches values of order $-\varepsilon^{2/3} |\log \varepsilon|$.

(p.81)

- If $\sigma > \sigma_c = \varepsilon^{1/2}$, then sample paths are likely to cross the unstable branch and



reach negative values of order 1 already for $y(t)$ of order $\sigma^{4/3}$. The probability that this does not happen is of order $e^{-O(\sigma^2/\varepsilon|\log\sigma|)}$.

Fig. 3.6: Stochastic dynamics near a saddle-node bifurcation, for $\varepsilon = 0.03$ and (a) $\sigma' = \sigma = 0.03 < \varepsilon^{1/2}$, and (b) $\sigma' = 0.25, \sigma = 0.35 > \varepsilon^{1/2}$. In both cases, the sample paths are likely to stay in the shaded set $\mathcal{B}(h)$, but for strong noise intensity, they may nevertheless overcome the unstable equilibrium branch before $y(t)$ reaches the bifurcation value.

Thus for $\sigma < \varepsilon^{1/2}$, the situation does not differ notably from the deterministic one: Sample paths feel the bifurcation after a delay of order $\varepsilon^{2/3}$, and then they quickly react by jumping to negative x of order 1. If $\sigma > \varepsilon^{1/2}$, on the other hand, noise induces a new behaviour: Sample paths feel the bifurcation some time before it happens, and thus anticipate the transition to negative x .

3.4.3 The Van der Pol oscillator

As a first illustration of how to patch together the above results in order to get the full picture of the dynamics of a slow–fast system, let us consider the van der Pol oscillator. This oscillator is based on an electric RCL circuit modelling the dynamics of a triode (van der Pol 1920, 1927). In the large-damping case, its dynamics is described by the slow–fast system

(3.47)

$$\begin{aligned}\varepsilon \dot{x} &= y + x - \frac{x^3}{3}, \\ \dot{y} &= -x.\end{aligned}$$

This system is equivalent, up to a scaling, to the Fitz Hugh–Nagumo equations with $\alpha=\gamma=0$.

The system (3.47) admits two stable and one unstable equilibrium branches, meeting at two saddle-node bifurcation points $\pm(1, -2/3)$. The nullcline is simply the axis $x=0$. A solution starting anywhere in the plane (except possibly near the unstable branch) will first quickly approach a stable equilibrium branch, which it then tracks at a distance of order ε . Upon reaching the neighbourhood of one of the bifurcation points, it will jump, after a small delay of order $\varepsilon^{2/3}$, to the other stable branch, which it then tracks until reaching the other bifurcation point, cf. Fig. 3.7(a). This alternation of slow and fast motions will repeat periodically, a behaviour that van der Pol called *relaxation oscillations* (van der Pol, 1926). In the (x,y) -plane, the orbits enclose an area $\mathcal{A}(\varepsilon) = \mathcal{A}(0) + \mathcal{O}(\varepsilon^{2/3})$ (Mishchenko and Rozov 1980, Jung et al. 1990).

Assume now that noise of intensity $\sigma/\sqrt{\varepsilon}$ is added to the fast variable x . The previous results show that as long as $\sigma < \sqrt{\varepsilon}$, typical sample paths merely fluctuate around the deterministic limit cycle. In particular, the area enclosed by

the cycles is concentrated around the deterministic value $\mathcal{A}(\varepsilon) = \mathcal{A}(0) + \mathcal{O}(\varepsilon^{2/3})$. When $\sigma > \sqrt{\varepsilon}$, however, typical cycles are smaller, by an amount of order $\sigma^{4/3}$, than $\mathcal{A}(0)$ (Berglund and Gentz 2002b), cf. Fig. 3.7(b).

One can also analyse the situation when only the slow variable y is subjected to an additive noise term of intensity σ' . Then, a similar transition between large and small cycles occurs at a threshold noise intensity of order $\varepsilon^{1/3}$ (Berglund and Gentz, 2005, Section 6.1.2).

Remark 3.12 As σ further increases, for fixed ε , transitions from one stable branch to the other occur earlier and earlier.

(p.82)

A particular regime, in which transitions are advanced and which can be studied in detail, is the quasi-static regime, in which ε and σ are both small, and satisfy a relation of the form $\varepsilon = e^{-\lambda/\sigma^2}$, where λ is a parameter. (Note that this implies

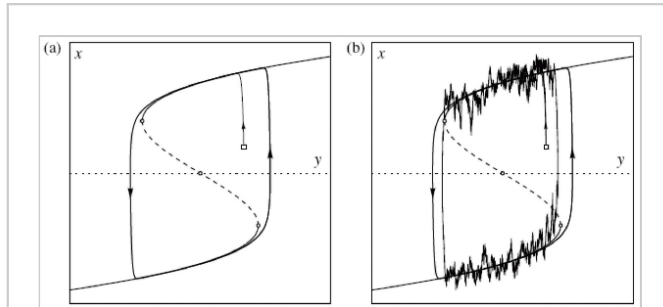


Fig. 3.7: (a) An orbit of the van der Pol oscillator for $\varepsilon = 0.02$. It quickly converges to a limit cycle. (b) When sufficiently strong noise is added to the fast variable x (here $\sigma = 0.3$), sample paths perform noisy cycles which are likely to be a little smaller than the deterministic cycle.

$\sigma = [\lambda/\log(\varepsilon^{-1})]^{1/2} \gg \sqrt{\varepsilon}$.) In that case, for small σ , ε is extremely small and one can consider the slow variable y locally as frozen. This permits one to examine the behaviour of the one-dimensional equation for x , with methods from the theory of large deviations (Freidlin, 2001).

Let $V_{yo}(x) = -y_0 x - \frac{1}{2}x^2 + \frac{1}{12}x^4$ be the double-well potential associated with the frozen system. If the depth of the potential well in which the frozen system is currently sitting is below $\lambda/2$, the state jumps to the other potential well after a time of order $1/\varepsilon$. For values of λ in a certain range, this leads to quasi-deterministic cycles which are smaller, by an amount of order 1, than the cycles obtained without noise.

3.5 Excitability

One of the interesting features of action-potential generation, reproduced by simple slow–fast models, is the phenomenon of *excitability*. A system is excitable if it admits an asymptotically stable equilibrium point, with the

particular feature that some orbits passing close by make a large excursion in phase space before returning to the point. In such a case, a small change of the vector field, controlled for instance by a bifurcation parameter, may produce a stable periodic orbit of large amplitude. Noise can have the same effect as a change of the bifurcation parameter, and occasionally move the system away from the stable equilibrium point and towards the periodic orbit. The system then makes a large excursion in phase space, corresponding to a spike, before returning to rest (Longtin, 2000, Kosmidis and Pakdaman, 2003) (see also Chapter 4).

(p.83) Various types of excitability can be distinguished (Izhikevich, 2000). One possible distinction concerns the period of the periodic orbit:

- In excitability of type I, the period of the orbit diverges as the bifurcation parameter approaches its threshold. It occurs for instance in the case of a saddle-node-to-invariant-circle (SNIC) bifurcation.
- In excitability of type II, the period of the orbit converges to a finite value as the bifurcation parameter approaches its threshold. It occurs for instance in the case of a Hopf bifurcation.

3.5.1 Excitability of type I

Excitability of type I occurs for instance when the nullcline $g(x,y) = 0$ intersects both the stable and unstable equilibrium branch near a saddle-node bifurcation point (in addition to a second intersection with the unstable branch further away). When the nullcline is moved towards the bifurcation point, the two intersection points collapse, and their unstable manifolds are replaced by a periodic orbit. This situation occurs, for instance, in the Morris–Lecar model, when the parameter x_4 is sufficiently small for the nullcline to be close to a step function.

The dynamics in the vicinity of the bifurcation point can be described by the normal form

(3.48)

$$\begin{aligned}\varepsilon \dot{x} &= y - x^2, \\ \dot{y} &= \delta - y.\end{aligned}$$

The parameter δ measures the distance to the saddle-node-to-invariant-circle bifurcation. There are two equilibrium branches, a stable one given by $x_-^*(y) = \sqrt{y}$ and an unstable one given by $x_+^*(y) = -\sqrt{y}$. If $\delta > 0$, the nullcline $y = \delta$ intersects the equilibrium branches at $(\sqrt{\delta}, \delta)$, which is an asymptotically stable node, and at $(-\sqrt{\delta}, \delta)$, which is a saddle. If $\delta < 0$, the invariant line $y = \delta$ represents the portion of the periodic orbit lying near the origin (this orbit can only be reproduced when including more nonlinear terms in the normal form).

The invariant curve $x = \bar{x}_-(y, \varepsilon)$, tracking the stable equilibrium branch for larger y , converges to the stable node $(\sqrt{\delta}, \delta)$ as y converges to δ , cf. Fig. 3.8. It has an expansion of the form

(3.49)

$$\bar{x}_-(y, \varepsilon) = \sqrt{y} + \varepsilon \frac{y - \delta}{4y} + \dots.$$

One can also define an invariant curve $x = \bar{x}_+(y, \varepsilon)$ tracking the unstable equilibrium branch. It coincides with the stable manifold of the saddle point $(-\sqrt{\delta}, \delta)$, while the unstable manifold of the saddle consists of the part of the nullcline $y = \delta$ below the stable node (Fig. 3.8).

(p.84)

Consider now the situation where noise is added to the fast variable, i.e. the stochastic differential equation

(3.50)

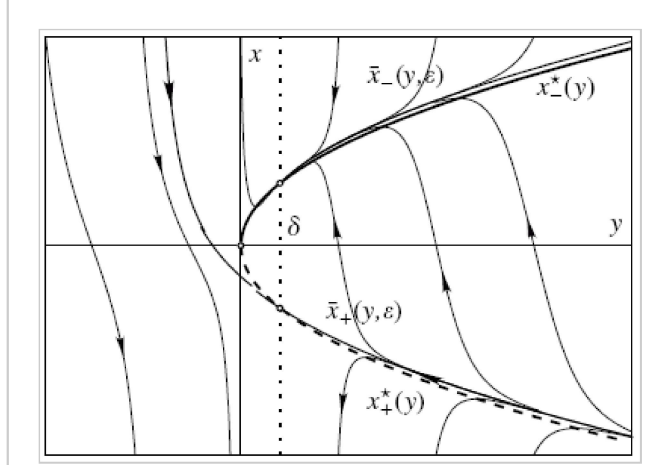


Fig. 3.8: Some orbits of the deterministic slow–fast system (3.48) for $\delta = 0.2$ and $\varepsilon = 0.1$. The curve $x = \bar{x}_+(y, \varepsilon)$, tracking the unstable equilibrium branch $x = x^*_+(y)$, is also the stable manifold of the saddle point $(-\sqrt{\delta}, \delta)$. The unstable manifold of the saddle is contained in the nullcline (dotted line).

$$\begin{aligned} dx(t) &= \frac{1}{\varepsilon}(y(t) - x(t)^2)dt + \frac{\sigma}{\sqrt{\varepsilon}}F(x(t), y(t))dW_t, \\ dy(t) &= (\delta - y(t))dt, \end{aligned}$$

where we assume that $F(x, y)$ is bounded away from zero. In fact, the equation for the slow variable is closed and can be solved:

(3.51)

$$y(t) = \delta + (y(0) - \delta)e^{-t}.$$

The system is thus equivalent to the one-dimensional time-dependent equation

$$dx(t) = \frac{1}{\varepsilon}(\delta + (y(0) - \delta)e^{-t} - x(t)^2)dt + \frac{\sigma}{\sqrt{\varepsilon}}F(x(t), \delta + (y(0) - \delta)e^{-t})dW_t.$$

In particular, if $y(0)=\delta$, we simply have the autonomous equation

(3.53)

$$dx(t) = \frac{1}{\varepsilon}(\delta - x(t)^2)dt + \frac{\sigma}{\sqrt{\varepsilon}}F(x(t), \delta)dW_t,$$

describing the overdamped motion of a particle in the static potential

$V(x) = \frac{1}{3}x^3 - \delta x$. This potential has a local minimum at $x = \sqrt{\delta}$ and a local maximum (p.85) at $x = -\sqrt{\delta}$, with a potential difference $\frac{4}{3}\delta^{3/2}$. We thus know that if $\sigma \ll \delta^{3/4}$, sample paths will be trapped near the potential minimum for a time of order $e^{\text{const}\delta^{3/2}/\sigma^2}$. Furthermore, it is known (Day, 1983, Bovier *et al.*, 2004) that for small noise intensity, the law of the escape time is well approximated by an exponential distribution.

If the sample path starts at some $y(0)>\delta$, one can proceed as in the stable case by defining a neighbourhood $B(h)$ of the deterministic invariant curve $x=\bar{x}_-(y, \varepsilon)$. Similar computations as in Section 3.2 show that $\mathcal{B}(h)$ has a width scaling like $h/y^{1/4}$. If $\sigma \ll \delta^{3/4}$, sample paths are likely to remain in $\mathcal{B}(h)$ for exponentially long time spans, as in the case $y(0)=\delta$, provided we choose $h \ll \sigma$. Otherwise, sample paths are likely to overcome the unstable equilibrium branch as soon as $\mathcal{B}(\sigma)$ reaches a width of order \sqrt{y} , that is, when $y(t)$ is of order $\sigma^{4/3}$. By (3.51), this happens at a time of order $|\log\sigma|$, cf. Fig.3.9.

Let us now implement this local analysis into the context of the full system (e.g. the Morris–Lecar equations, cf. Fig. 3.10). The parameter δ of the normal form can be computed by expanding the slow component of the vector field around the saddle–node bifurcation point (x^*, y^*) , yielding

(3.54)

$$\delta \simeq \frac{g(x^*, y^*)}{\partial_y g(x^*, y^*)}.$$

From the previous analysis, one concludes that

- If $\sigma^{3/4}$, the system will display rare spikes, with approximately exponentially distributed waiting times between spikes (i.e. the spike times follow a Poisson process), with mean of order $e^{\text{const}\delta^{3/2}/\sigma^2}$.

(p.86)

- If $\sigma \geq \delta^{3/4}$, the system will spike frequently, the time interval between spikes being of order $|\log\sigma|$ because of the time needed to

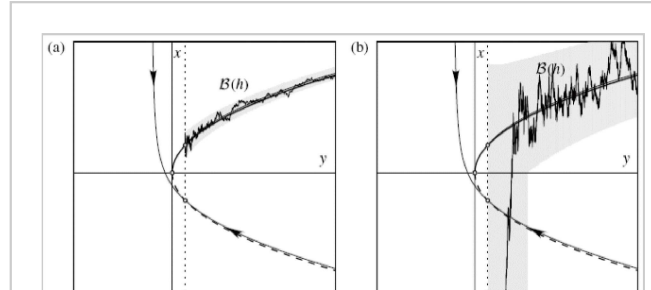


Fig. 3.9: Sample paths of the stochastic differential equation (3.50) for $\delta = \varepsilon = 0.1$, and (a) $\sigma = 0.05 < \delta^{3/4}$, (b) $\sigma = 0.35 > \delta^{3/4}$. In both cases, the sample

reach the active zone, in which escape from the local potential minimum is easy.

Fig. 3.11 illustrates these results for different values of the noise intensity. We expect that this picture will not change significantly when weak noise of intensity σ' is added to the slow variable y , as long as $\sigma' \ll \delta$. For stronger noise, there is the possibility that the system escapes from the stable equilibrium point by turning around the saddle-node bifurcation point.

paths are likely to stay in the shaded set $\mathcal{B}(h)$, but for strong noise intensity, they are likely to overcome the unstable equilibrium branch before reaching the stable equilibrium point.

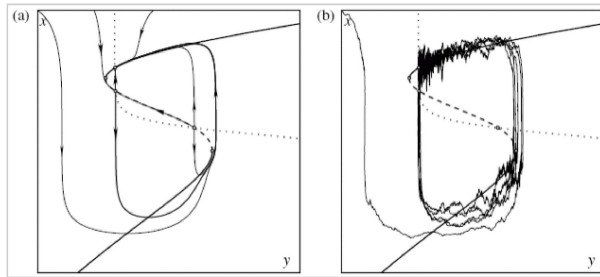


Fig. 3.10: (a) Some orbits of the deterministic Morris–Lecar model. Parameter values are $x_1 = 0.5$, $x_2 = 0.15$, $x_3 = 0.37$, $x_4 = 0.05$, $c_1 = 4.75$, $c_2 = 1$, $c_3 = 5$, $V_2 = 2$, $V_3 = 0$ and $\varepsilon = 0.05$. We show in particular the stable and unstable manifolds of the hyperbolic equilibrium point. Its unstable manifolds both converge to the same stable equilibrium point, but have very different lengths. (b) A sample path of the Morris–Lecar model with the same parameter values as before, and noise of intensity $\sigma = 0.07$ and $\sigma' = 0.05$ added to the slow and fast components, respectively.

3.5.2 Excitability of type II

Excitability of type II occurs for instance when the nullcline $g(x,y)=0$ intersects only the stable equilibrium branch near a saddle–node bifurcation point. This situation occurs, e.g. in the FitzHugh–Nagumo model, when $\beta=1$, $\gamma=0$ and $\alpha = 1/\sqrt{3} + \delta$ for small δ : Then the nullcline is the horizontal line $x = 1/\sqrt{3} + \delta$, passing at a distance δ above one of the saddle-node bifurcation points.

The dynamics near the bifurcation point can again be understood through its normal form, given by

(3.55)

$$\begin{aligned}\varepsilon \dot{x} &= y - x^2, \\ \dot{y} &= \delta - x.\end{aligned}$$

As before, this system has two equilibrium branches at $x = \pm\sqrt{y}$. The associated invariant curves are shown in Fig. 3.12. Unlike in the case discussed in the (p.87) previous section, there is only a single equilibrium point (δ, δ^2) . The linearization of the vector field at this point is given by the matrix

(3.56)

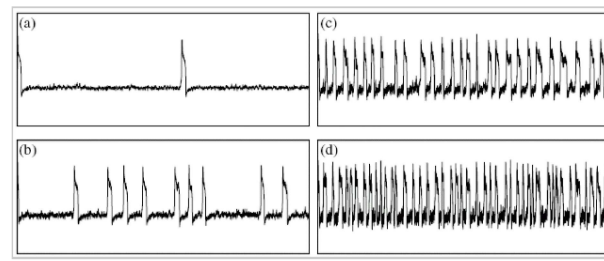


Fig. 3.11: Plot of $-x(t)$ as a function of t for the Morris–Lecar model, showing the different spiking behaviours as the noise intensity increases. Parameter values are the same as in Fig. 3.10, except that $c_1 = 4.7$ and (a) $\sigma = 0.027$, (b) $\sigma = 0.045$, (c) $\sigma = 0.085$, and (d) $\sigma = 0.125$. The behaviour changes from rare random spikes roughly following a Poisson process to frequent, more regularly distributed spikes. For stronger noise, the spikes become irregular again because multiple transitions between equilibrium branches are more likely.

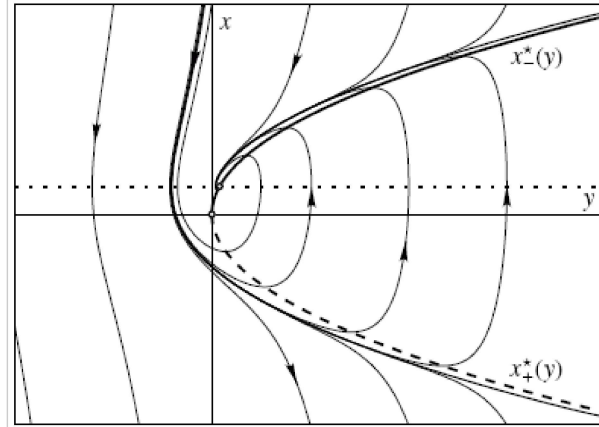


Fig. 3.12: Some orbits of the deterministic slow–fast system (3.55) for $\varepsilon = \delta = 0.2$. The invariant curve tracking the unstable equilibrium branch $x = x^*_-(y)$ for positive y delimits the basin of attraction of the stable equilibrium point (δ, δ^2) .

$$A = \begin{pmatrix} -2\delta/\varepsilon & 1/\varepsilon \\ -1 & 0 \end{pmatrix},$$

(p.88) which has eigenvalues $(-\delta \pm \sqrt{\delta^2 - \varepsilon})/\varepsilon$. Thus the equilibrium point is a stable node for $\delta > \sqrt{\varepsilon}$, a stable focus for $0 < \delta < \sqrt{\varepsilon}$, an unstable focus for

$-\sqrt{\varepsilon} < \delta < 0$ and an unstable node for $\delta < -\sqrt{\varepsilon}$. At $\delta = 0$, the point undergoes a Hopf bifurcation. It is known that such a bifurcation generically corresponds to either the creation of a stable periodic orbit, or the destruction of an unstable periodic orbit. In the present case, a stable periodic orbit is created as δ becomes negative. This orbit has a very particular shape: Starting near the origin, it tracks the unstable equilibrium branch for some time, then quickly jumps to the stable equilibrium branch, which it tracks until returning near the origin, closing the cycle.

Placing this local analysis back into the context of the FitzHugh–Nagumo equations, one sees that

- For $\delta > 0$, all orbits converge to the stable equilibrium point, cf. Fig. 3.13(a).
- As δ becomes negative, the system develops a periodic orbit of particular shape, reminding some authors of the shape of a duck, cf. Fig. 3.13(b). This is why these solutions are often called (French) ducks, or canards (Callot, Diener and Diener, 1978, Eckhaus, 1983).

Canards only exist in an interval of δ -values which is exponentially small in ε . Decreasing δ further, the periodic orbit quickly starts resembling that of the van der Pol oscillator.

Let us now add noise to the system, first by considering only the normal form

(3.57)

$$\begin{aligned} dx(t) &= \frac{1}{\varepsilon}(y(t) - x(t)^2)dt + \frac{\sigma}{\sqrt{\varepsilon}}dW_t^{(1)}, \\ dy(t) &= (\delta - x(t))dt + \sigma'dW_t^{(2)}. \end{aligned}$$

(p.89) Unlike in the case studied in the previous section, we cannot reduce the system to a one-dimensional one, which makes its analysis much harder. In particular, we now have to study where and when sample paths cross the invariant curve tracking the unstable equilibrium branch, which delimits the basin of attraction of the stable

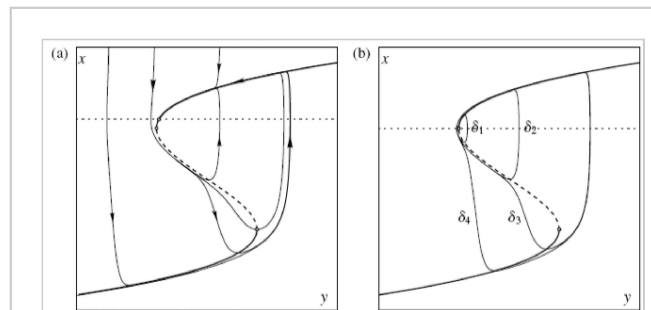


Fig. 3.13: (a) Orbits of the FitzHugh–Nagumo system for $\varepsilon = 0.05$, $\beta = 1$, $\gamma = 0$ and $\alpha = 1/\sqrt{3} + \delta$, with $\delta = 0.1$. The orbit tracking the unstable equilibrium branch has been obtained by starting in the lower right saddle-node bifurcation point, and going backwards in time. (b) Periodic orbits of the same system, for negative δ , taking values $\delta_1 = 0.003$, $\delta_2 = 0.003765458$, $\delta_3 = 0.003765459$ and $\delta_4 = 0.005$.

equilibrium point (Fig. 3.14).

If $\delta > \sqrt{\varepsilon}$, the equilibrium point (δ, δ^2) is a node, towards which the invariant curve tracking the stable branch converges from the right. We can basically repeat the analysis from the previous section (with δ replaced by δ^2), showing that

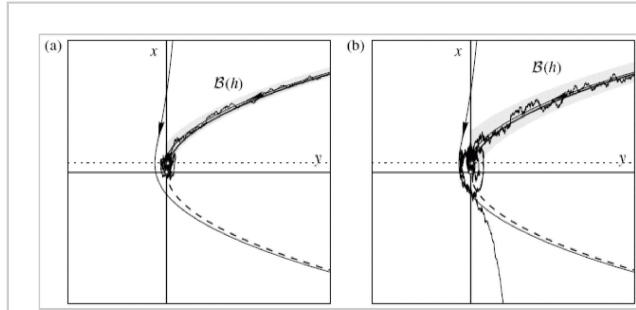


Fig. 3.14: Sample paths of the stochastic differential equation (3.57) for $\varepsilon = \delta = 0.1$, and (a) $\sigma = 0.05$, $\sigma' = 0.02$ and (b) $\sigma = 0.08$, $\sigma' = 0.02$. In both cases, the sample paths are likely to stay in the shaded set $\mathcal{B}(h)$, but for strong noise intensity, they are likely to cross the invariant curve tracking the unstable branch.

- If $\sigma \ll \delta^{3/2}$, the system will display rare spikes, with approximately exponentially distributed waiting times between spikes (i.e. the spike times follow a Poisson process) with mean waiting time of order $e^{\text{const} \delta^3 / \sigma^2}$, cf. Fig. 3.15(a).
- If $\sigma \geq \delta^{3/2}$, the system will spike frequently, the time interval between spikes being of order $|\log \sigma|$ because of the time needed to reach the active zone, in which escape from the local potential minimum is easy, cf. Fig. 3.15(b).

If $\delta < \sqrt{\varepsilon}$, the equilibrium point (δ, δ^2) is a focus, around which the invariant curve coming from the right is wound. This situation has been analysed using an approximate constant of motion of the normal form. The result of a rather intricate scaling analysis (Muratov and Vanden-Eijnden, 2008) is that there are now three different regimes, namely

- If $\sigma^2 + (\sigma')^2 \ll (\delta \varepsilon^{1/4})^2$, escape from the stable focus is unlikely, and the system will display rare spikes. The average time elapsing between spikes has order $e^{-(\delta \varepsilon^{1/4})^2 / (\sigma^2 + (\sigma')^2)}$.

(p.90)

- If $(\delta \varepsilon^{1/4})^2 \ll \sigma^2 + (\sigma')^2 \ll \delta \varepsilon$, escape from the focus is still unlikely, but there is a certain chance that a spike will

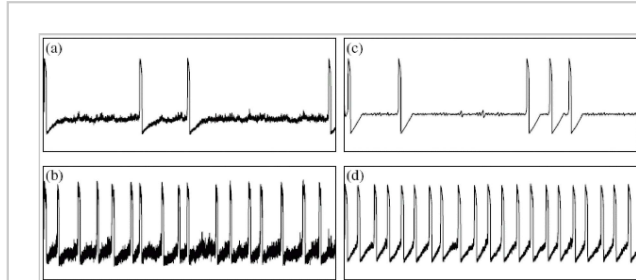


Fig. 3.15: Plot of $-x(t)$ as a function of t for the FitzHugh–Nagumo model, showing the different spiking behaviours. Parameter values are $\varepsilon = 0.01$

immediately be followed by another one, so that the system

displays rare sequences of spikes, cf. Fig. 3.15(c).

and (a) $\delta = 0.15$, $\sigma = \sigma' = 0.04$, (b) $\delta = 0.15$, $\sigma = \sigma' = 0.15$, (c) $\delta = 0.01$, $\sigma = \sigma' = 0.003$, and (d) $\delta = 0.01$, $\sigma = \sigma' = 0.05$.

- If $\sigma^2 + (\sigma')^2 \gg \delta\epsilon$, the system again displays frequent and more regularly spaced spikes, cf. Fig. 3.15(d).

We did not discuss the distribution of time intervals between spikes, for the reason that not much is known about it. Unlike the case of exit from a potential well, we have to deal here with the problem of noise-induced escape through a characteristic boundary (Day, 1990 *a*, 1992), which does not necessarily follow an exponential law. If, for instance, the boundary is a periodic orbit, *cycling* occurs and the exit location depends logarithmically on the noise intensity (Day, 1990 *b*, 1994, 1996, Berglund and Gentz, 2004). This is related to the fact that a characteristic boundary is not crossed instantaneously the moment a small neighbourhood is reached.

Finally note that the quasi-static regime of exponentially small ϵ (Freidlin, 2001) can also be treated in this particular situation (DeVille, Vanden-Eijnden and Muratov 2005, Muratov, Vanden-Eijnden and E, 2005, Sowers 2008).

3.6 Concluding remarks

We have shown how to determine the effects of noise on slow–fast differential equations, such as those appearing in models for action-potential generation through neuron membranes. The analysis proceeds by studying separately the dynamics near stable and unstable equilibrium branches, near bifurcation points, and in the remaining phase space, before patching the parts together in order to obtain the global picture.

The dynamics away from bifurcation points is well understood, under very general assumptions. Near bifurcation points, the analysis has to rely on case (**p.91**) studies, and not all cases have yet been described to the same level of accuracy. In particular, in situations leading to excitability of type II (a nullcline intersecting a stable branch near a saddle-node bifurcation point), the relevant scaling regimes have been determined, but little is known on the distribution of exit times. The stochastic dynamics near bifurcation points of higher codimension has also not yet been analysed in sufficient detail.

The models we have considered here, although being relatively simple, are able to reproduce several types of spiking behaviour observed in experiments: rare isolated spikes, frequent, nearly periodic spikes, and rare clusters of spikes (bursts). Comparing the predictions of these theoretical models with

experimental results will allow one to determine the noise intensities to be used in the stochastic model equations, thereby improving their accuracy.

Acknowledgement

Support by the German Research Council (DFG), within the CRC 701 ‘Spectral Structures and Topological Methods in Mathematics’, is gratefully acknowledged.

References

Bibliography references:

- Benôit, E. (ed.) (1991). *Dynamic Bifurcations*, Berlin. Springer-Verlag.
- Berglund, N. and Gentz, B. (2002a). Beyond the Fokker–Planck equation: Pathwise control of noisy bistable systems. *J. Phys. A*, **35**(9), 2057–2091.
- Berglund, N. and Gentz, B. (2002b). The effect of additive noise on dynamical hysteresis. *Nonlinearity*, **15**(3), 605–632.
- Berglund, N. and Gentz, B. (2002c). Pathwise description of dynamic pitchfork bifurcations with additive noise. *Probab. Theory Related Fields*, **122**(3), 341–388.
- Berglund, N. and Gentz, B. (2002d). A sample-paths approach to noise-induced synchronization: Stochastic resonance in a double-well potential. *Ann. Appl. Probab.*, **12**, 1419–1470.
- Berglund, N. and Gentz, B. (2003). Geometric singular perturbation theory for stochastic differential equations. *J. Differential Equations*, **191**, 1–54.
- Berglund, N. and Gentz, B. (2004). On the noise-induced passage through an unstable periodic orbit I: Two-level model. *J. Statist. Phys.*, **114**, 1577–1618.
- Berglund, N. and Gentz, B. (2005). *Noise-Induced Phenomena in Slow–Fast Dynamical Systems. A Sample-Paths Approach*. Probability and its Applications. Springer-Verlag, London.
- Berglund, N. and Kunz, H. (1999). Memory effects and scaling laws in slowly driven systems. *J. Phys. A*, **32**(1), 15–39.
- Bovier, A., Eckhoff, M., Gayrard, V., and Klein, M. (2004). Metastability in reversible diffusion processes. I. Sharp asymptotics for capacities and exit times. *J. Eur. Math. Soc. (JEMS)*, **6**(4), 399–424.
- Callot, J.-L., Diener, F., and Diener, M. (1978). Le problème de la “chasse au canard”. *C. R. Acad. Sci. Paris Sér. A-B*, **286**(22), A1059–A1061.

(p.92) Day, M. (1990a). Large deviations results for the exit problem with characteristic boundary. *J. Math. Anal. Appl.*, **147**(1), 134–153.

Day, M. V. (1983). On the exponential exit law in the small parameter exit problem. *Stochastics*, **8**, 297–323.

Day, M. V. (1990b). Some phenomena of the characteristic boundary exit problem. In *Diffusion processes and related problems in analysis, Vol. I (Evanston, IL, 1989)*, Volume 22 of *Progr. Probab.*, pp. 55–71. Birkhäuser Boston, Boston, MA.

Day, M. V. (1992). Conditional exits for small noise diffusions with characteristic boundary. *Ann. Probab.*, **20**(3), 1385–1419.

Day, M. V. (1994). Cycling and skewing of exit measures for planar systems. *Stochastics*, **48**, 227–247.

Day, M. V. (1996). Exit cycling for the van der Pol oscillator and quasipotential calculations. *J. Dynam. Differential Equations*, **8**(4), 573–601.

DeVille, R. E. L., Vanden-Eijnden, E., and Muratov, C. B. (2005). Two distinct mechanisms of coherence in randomly perturbed dynamical systems. *Phys. Rev. E* (3), **72**(3), 031105.

Eckhaus, W. (1983). Relaxation oscillations including a standard chase on French ducks. In *Asymptotic analysis, II*, Volume 985 of *Lecture Notes in Math.*, pp. 449–494. Springer, Berlin.

Fenichel, N. (1979). Geometric singular perturbation theory for ordinary differential equations. *J. Differential Equations*, **31**(1), 53–98.

FitzHugh, R. (1961). Impulses and physiological states in models of nerve membrane. *Biophys. J.*, **1**, 445–466.

Freidlin, M. I. (2001). On stable oscillations and equilibriums induced by small noise. *J. Statist. Phys.*, **103**, 283–300.

Grad ste in, I. S. (1953). Application of A. M. Lyapunov's theory of stability to the theory of differential equations with small coefficients in the derivatives. *Mat. Sbornik N. S.*, **32**(74), 263–286.

Haberman, R. (1979). Slowly varying jump and transition phenomena associated with algebraic bifurcation problems. *SIAM J. Appl. Math.*, **37**(1), 69–106.

Hodgkin, AL and Huxley, AF (1952, Aug). A quantitative description of membrane current and its application to conduction and excitation in nerve. *J. Physiol. (Lond.)*, **117**(4), 500–44.

- Izhikevich, E. M. (2000). Neural excitability, spiking and bursting. *Internat. J. Bifur. Chaos Appl. Sci. Engrg.*, **10**(6), 1171–1266.
- Jones, C. K. R. T. (1995). Geometric singular perturbation theory. In *Dynamical systems (Montecatini Terme, 1994)*, pp. 44–118. Springer, Berlin.
- Jung, P., Gray, G., Roy, R., and Mandel, P. (1990). Scaling law for dynamical hysteresis. *Phys. Rev. Letters*, **65**, 1873–1876.
- Kosmidis, E. K. and Pakdaman, K. (2003). An analysis of the reliability phenomenon in the FitzHugh-Nagumo model. *J. Comput. Neuroscience*, **14**, 5–22.
- Longtin, A. (2000). Effect of noise on the tuning properties of excitable systems. *Chaos, Solitons and Fractals*, **11**, 1835–1848.
- (p.93)** Mishchenko, E. F. and Rozov, N. Kh. (1980). *Differential equations with small parameters and relaxation oscillations*. Plenum Press, New York.
- Morris, C and Lecar, H (1981, Jul). Voltage oscillations in the barnacle giant muscle fiber. *Biophys J*, **35**(1), 193–213.
- Muratov, C. B. and Vanden-Eijnden, E. (2008). Noise-induced mixed-mode oscillations in a relaxation oscillator near the onset of a limit cycle. *Chaos* (18), 015111.
- Muratov, C. B., Vanden-Eijnden, E., and E, W. (2005). Self-induced stochastic resonance in excitable systems. *Phys. D*, **210**(3-4), 227–240.
- Nagumo, J. S., Arimoto, S., and Yoshizawa, S. (1962). Active pulse transmission line simulating nerve axon. *Proc. IRE*, **50**, 2061–2070.
- Nayfeh, A. H. (1973). *Perturbation methods*. John Wiley, New York.
- Øksendal, B. (1985). *Stochastic Differential Equations*. Springer-Verlag, Berlin.
- O'Malley, Jr., R. E. (1974). *Introduction to Singular Perturbations*. Academic Press, New York.
- O'Malley, Jr., R. E. (1991). *Singular Perturbation Methods for Ordinary Differential Equations*, Volume 89 of *Applied Mathematical Sciences*. Springer-Verlag, New York.
- Pontryagin, L. S. (1957). Asymptotic behavior of solutions of systems of differential equations with a small parameter in the derivatives of highest order. *Izv. Akad. Nauk SSSR. Ser. Mat.*, **21**, 605–626.

Sowers, R. B. (2008). Random perturbations of canards. *J. Theoret. Probab.*, **21**, 824–889.

Tikhonov, A. N. (1952). Systems of differential equations containing small parameters in the derivatives. *Mat. Sbornik N. S.*, **31**, 575–586.

van der Pol, B. (1920). A theory of the amplitude of free and forced triode vibration. *Radio. Rev.*, **1**, 701.

van der Pol, B. (1926). On relaxation oscillation. *Phil. Mag.*, **2**, 978–992.

van der Pol, B. (1927). Forced oscillations in a circuit with non-linear resistance. (Reception with reactive triode). *Phil. Mag.*, **3**, 65–80.

Wasow, W. (1987). *Asymptotic Expansions for Ordinary Differential Equations*. Dover Publications Inc., New York. Reprint of the 1976 edition.

Notes:

(1) \mathcal{M}_ε is called *invariant under the flow*, if $(x(0), y(0)) \in \mathcal{M}_\varepsilon$ implies that $(x(t), y(t)) \in \mathcal{M}_\varepsilon$ as long as $y(t) \in I$ holds.

(2) The notation $a(y, \varepsilon) \asymp b(y, \varepsilon)$ means that two functions a and b behave in the same way, in the sense that $a(y, \varepsilon)/b(y, \varepsilon)$ is bounded above and below by positive constants, independent of y and ε .

PRINTED FROM OXFORD SCHOLARSHIP ONLINE (www.oxfordscholarship.com). (c) Copyright Oxford University Press, 2018. All Rights Reserved. Unsingle chapter of a monograph in OSO for personal use (for details see www.oxfordscholarship.com/page/privacy-policy). Subscriber: University of Edinburgh;



Access brought to you by: